RESEARCH PAPER

Degradation of perfluorooctanoic acid by zero-valent iron nanoparticles under ultraviolet light

Chunjie Xia · Jia Liu

Abstract Perfluorooctanoic acid (PFOA) is ubiquitous in the environment because of its wide applications in aqueous film forming foam, food packing, waterproof breathable fabrics, and Teflon products. Though it is resistant to biodegradation, photocatalytic degradation has been proven possible. In this study, zero-valent iron nanoparticles (Fe^0 NPs), with or without 1% polyvinyl-pyrrolidone (PVP) coating, were used for PFOA degradation under ultraviolet C (UVC) light for the first time. PFOA was degraded faster initially (e.g., < 13 h) with Fe^0 NPs than without Fe^0 NPs under UVC light. In addition, the degradation rate using Fe^0 NPs without coating was higher than that with 1% PVP coating in the initial 6 h, although the difference was diminished afterwards. Both Fe^{2+} and Fe^{3+} ions were detected during the process. Shorter-chain perfluorocarboxylic acids (PFCAs), i.e., PFHpA, PFHxA, PFPeA, and PFBA, were detected as main intermediates; fluoride ions (F^-) were also detected. Rapid consumption of Fe^{3+} (plus the lower UV–vis absorption intensity observed for a mixture of PFOA and $FeCl_3$ compared to the intensity observed for $FeCl_3$ alone) indicated the possible formation of $[C7F15COO-Fe]^{2+}$—a degradable complex. The UV/Fe^0 system is superior, with low toxicity of iron and no introduction of other chemicals. Additionally, the cost of Fe^0 NPs is low, and the recycle of Fe^0 NPs is easy from the treated water by their magnetic properties. The study provided an innovative, environment-friendly, and low-cost method for PFOA degradation by Fe^0 NPs under UVC light, which could be potentially applied for treatment of surface water and groundwater contaminated by PFOA.

Introduction

Per- and polyfluoroalkyl substances (PFAS), typically perfluorooctanoic acid (PFOA) and perfluorooctanesulfonic acid (PFOS), are ubiquitous in the environment, e.g., surface water, groundwater, sediment, soil, sludge, and air (Buck et al. 2011; Giesy and Kannan 2002; Houde et al. 2011; Houtz et al. 2013; Xiao 2017), and have received global attention because of their persistence, bioaccumulation potential, and possible adverse effects on living organisms (Ahrens and Bundschuh 2014; Ahrens 2011). Therefore, removal of PFAS from contaminated environmental media is critically important.

Several water treatment technologies have been applied for PFOA removal, such as coagulation, sand filtration, adsorption (e.g., activated carbon), anion exchange, and

C. Xia · J. Liu
Department of Civil and Environmental Engineering, Southern Illinois University, 1230 Lincoln Dr, Carbondale, IL 62901, USA

J. Liu (✉)
Materials Technology Center, Southern Illinois University, 1245 Lincoln Dr, Carbondale, IL 62901, USA
e-mail: jialiu@siu.edu

membrane filtration (Takagi et al. 2011; Eschauzier et al. 2012; Flores et al. 2013; Ye et al. 2019a; Ye et al. 2019b). However, these technologies are based on physical removal processes, and the removed (e.g., by adsorption) PFOA still requires further degradation. The best way is to develop a method that can degrade PFOA to harmless species. Due to the very strong C–F bond, PFOA cannot be degraded even by advanced oxidation under mild conditions (Schröder and Meesters 2005). In the last decades, several methods have been developed for PFOA degradation, such as sonolysis (Moriwaki et al. 2005; Cheng et al. 2008; Fernandez et al. 2016), persulfate oxidation (Bruton and Sedlak 2018), electrochemical treatment (Schaefer et al. 2015), ultraviolet (UV) photolysis (Chen et al. 2007; Giri et al. 2011), and photocatalysis (Giri et al. 2011; Chen and Zhang 2006; Wang et al. 2008; Gomez-Ruiz et al. 2018; Li et al. 2013; Zhao and Zhang 2009). A composite of titanium dioxide (TiO_2) and reduced graphene oxide (rGO) (Gomez-Ruiz et al. 2018), indium oxide (In_2O_3) nanoparticles (NPs) (Li et al. 2013), and β-gallium oxide (β-Ga_2O_3) NPs (Zhao and Zhang 2009) have been used as heterogeneous photocatalysts for PFOA photocatalytic degradation (Wang et al. 2017). In addition, Fe^{3+} has been proven effective in mediating PFOA degradation under both UVC (185 nm or 254 nm) and natural light (Wang et al. 2008; Wang et al. 2017); the degradation and defluorination percentages were 78.9% and 38.7% within 4 h under 254 nm, respectively, and 97.8% and 12.7% in 28 days under natural light, respectively. PFOA ($C_7F_{15}COOH$) degradation was initiated by possible light-induced electron transfer, by forming a complex of $[C_7F_{15}COO\text{-}Fe]^{2+}$ from Fe^{3+} and the dissociated perfluorooctanoate anion $C_7F_{15}COO^-$ (PFO^-) (Wang et al. 2008; Jin et al. 2014). Besides, the UV-Fenton process—using the UV/Fe^{2+}/H_2O_2 system was reported to degrade PFOA efficiently: the defluorination process was mainly due to the interactions between PFOA and Fe^{3+} ions (Tang et al. 2012). However, by introducing Fe^{3+} with iron salts during the water treatment processes, anions such as SO_4^{2-}, Cl^-, and NO_3^- were also brought into the system, which may unnecessarily increase the ionic content in the ecosystem—for example, increase the soil salinity (Zhao et al. 2019).

Zero-valent iron (Fe^0) appears then as an alternative to iron salts, which inclusively presents better performance in the degradation of a variety of organic contaminants (Gehrke et al. 2015). Elemental iron has been proved by the U.S. Food and Drug Administration for biocompatibility test. A previous study also showed a biphasic response—a manifestation of hormesis

(Iavicoli et al. 2018) of bacteria cells exposed to Fe^0 NPs: at relatively low concentrations of 1–100 mg/L of Fe^0 (aged 2 weeks), there was beneficial impact on bacterial growth; however, under higher concentrations of Fe^0, i.e., > 100 mg/L, dosage-dependent toxicity began to show from reduced bacteria concentration (Liu et al. 2013b; Liu and Vipulanandan 2013). In addition, the cost of Fe^0 NPs is relatively low at ~ $1–25/kg for sizes of 35–100 nm (Alibaba Group). A few studies have tried to use bare Fe^0 NPs to remove PFOA from contaminated water in the dark, resulting in less than 20% PFOA removal (Arvaniti et al. 2015; Lawal and Choi 2018). The main mechanisms for PFOA removal in those studies were adsorption and Fe-complexation, although a trace amount of fluoride ions (F^-) was observed in one removal process (Arvaniti et al. 2015; Lawal and Choi 2018; Park et al. 2018). However, bare Fe^0 NPs are easy to aggregate and oxidize; therefore, 1% PVP was used to prevent aggregation of Fe^0 NPs, so that the particles would have higher surface area, which would potentially endow them with higher surface reactivity (Mark and Wiesner 2017). Besides, the 1% PVP coating was used to lower the degree of oxidation of bare Fe^0 NPs, so that the particles would be more stable and easier to store (Tian et al. 2020). However, the PVP coating may also block some reactive sites on the surface, e.g., prevent oxidation of Fe^0 to release ions. A low value of 1% was used in this study to explore the effect (i.e., positive or negative) of PVP coating on the PFOA degradation process.

In this study, both bare and 1% PVP-coated Fe^0 NPs were used for PFOA photocatalytic degradation under UVC light for the first time. Different light conditions (i.e., UVC and visible light) for PFOA degradation were also studied. PFOA degradation by the UV/Fe^0 system was compared to that by the UV/Fe^0/H_2O_2 system. Besides, to elucidate the mechanism of PFOA removal, intermediates formed during the degradation process were analyzed. It was anticipated that Fe^0 NPs would be oxidized to Fe^{3+} in the presence of oxygen (Dutta et al. 2014; Bautitz et al. 2012; Laine et al. 2008), then the oxidized Fe^{3+} would form the $[C_7F_{15}COO\text{-}Fe]^{2+}$ complex for initiating PFOA photocatalytic degradation under UVC light (Wang et al. 2008; Jin et al. 2014). In comparison, PFOA would not be degraded under visible light or in the dark. It was also interesting to study whether the addition of H_2O_2 would enhance PFOA degradation in the UV/Fe^0 system like in the UV/Fe^{2+}/H_2O_2 system, or would bring no beneficial effect since

PFOA could not be defluorinated by hydroxyl radicals ·OH generated during photolysis of H_2O_2 (Javed et al. 2020).

Materials and methods

In general, PFOA degradation was tested in both UV/Fe^0 and UV/Fe^0/H_2O_2 systems. Both bare and 1% PVP-coated Fe^0 NPs were used. PFOA degradation under UVC (254 nm) light alone was used as the control. Fe^{2+} and Fe^{3+} ions, fluoride ions (F^-), and degradation intermediates were quantified during the process.

Chemicals

PFOA, cetyl trimethylammonium bromide (CTAB), and $NaBH_4$ were purchased from Sigma-Aldrich. M8-PFOA, the mixed standards of PFOA, perfluoroheptanoic acid (PFHpA), perfluorohexanoic acid (PFHxA), perfluoropentanoic acid (PFPeA), and perfluorobutanoic acid (PFBA), were provided by Wellington Laboratories Inc., Canada. $FeSO_4 \cdot 7H_2O$, $NH_3OH \cdot HCl$, H_2O_2, acetone (ACS grade), and methanol (Optima™ LC/MS grade) were purchased from Fisher Scientific. Alizarin fluorine blue, CH_3COOH, CH_3COONa, $La(NO_3)_3$, NaF, and Ferrozine ($C_{20}H_{12}N_4Na_2O_6S_2$) were purchased from Sigma-Aldrich. PVP-coated (1% w/w) Fe^0 NPs (35–45 nm) were purchased from U.S. Research Nanomaterials, Inc. Bare Fe^0 NPs were produced by the precipitation method (see Supporting Information) (Liu et al. 2013b). All water used in this study was deionized (D.I.) water except the Optima™ LC/MS-grade water for the mobile phase of liquid chromatography with tandem mass spectrometry (LC/MS/MS).

PFOA degradation experiments

Fe^0 NPs were sonicated at 20 kHz for 30 min (Sonics VC505, 500 W Ultrasonic Processor, Sonics & Materials, Inc., Newtown, CT, USA) for proper dispersion of the particles, and reached a final concentration of 100 mg/L in reactors. In comparison, H_2O_2 of 30 mM was added to the Fe^0 suspension. PFOA of 10 mg/L (or 1 mg/L) was loaded in quartz vials, which were rotated in a photoreactor (Luzchem, LZC-4X) equipped with 14 light bulbs (8 W each) to provide either UVC (254 nm) or visible light (Fig. S4 in Supporting Information). A high concentration of 10 mg/L of PFOA was chosen to clearly detect the intermediates formed during the entire degradation process. The light intensities of UVC and visible light were 6.57 mW/cm^2 and 22.0 mW/cm^2, respectively. The experiments were also performed in the dark by wrapping the vials with aluminum foil. PFOA degradation under UVC light without addition of Fe^0 NPs and H_2O_2 was used as the control. All experiments were performed at room temperature (i.e., 22 °C).

Analytical methods

PFOA sample preparation and analysis

During a 25-h irradiation period, 100 μL sample was taken constantly from each reaction vial using a gastight microsyringe, after vigorously shaking the vials. The sample was centrifuged at 14,000 rpm (i.e., 13,144g) (Eppendorf MiniSpin plus Microcentrifuge) in a 2-mL microcentrifuge tube for 20 min to separate the Fe^0 NPs from the suspension. Afterwards, an aliquot of 20 μL of the supernatant was transferred to 480 μL of methanol in a VWR® centrifugal filter with a 0.2-μm nylon membrane. M8-PFOA of 25 μL (1 mg/L) was spiked in the VWR filter as an internal standard. Then the filter was centrifuged at 3000 rpm (i.e., 604g) for 5 min. The filtered solution was transferred to a liquid chromatography vial by a glass Pasteur pipette, and capped with a pre-slit cap. In total, 5 samples (i.e., 500 μL) were taken from each vial, which equaled 5% of the whole sample volume in the vial. All experiments were conducted in duplicate.

An Agilent 1260 HPLC (Agilent Technologies, Santa Clara, CA) interfaced with a 3200 Q trap triple quadrupole/linear ion trap mass spectrometer (AB Sciex; Toronto, Canada) and with an electrospray ionization detector was used to determine the concentrations of PFOA and its degradation intermediates (Rhoads et al. 2008). The information on PFCA retention time and other MS parameters are given in Table S1 in Supporting Information. An Agilent column (ZORBAX Extend C18, 3.5 μm, 80 Å, 2.1 × 100 mm) was used for the PFCA analysis. The injection volume was 5 μL. The mobile phase was a mixture of 2 mM NH_4Ac in Optima™ LC/MS-grade water and 2 mM NH_4Ac in Optima™ LC/MS-grade methanol with a flow rate of 0.2 mL/min. The detailed LC mobile phase gradient for PFCA detection is shown in Table S2 in Supporting Information.

Analysis of fluoride ion (F⁻)

The concentration of fluoride ions (F⁻) was determined by a UV–vis spectrophotometer (Thermo Scientific, Biomate 3S) based on measuring the fluoride/lanthanum(III)/alizarin fluorine blue ternary complex at a wavelength of 620 nm, following the People's Republic of China's Environmental Protection Standards HJ 488-2009 (Environmental Protection Standard of China HJ 488-2009 2009; Shimada et al. 2005). In brief, a sample of 2 mL was transferred to a 25-mL volumetric flask, then 10 mL indicator—a mixture of alizarin fluorine blue solution (0.001 M), acetic acid–sodium acetate buffer solution (pH = 4.1), acetone, and lanthanum nitrate solution (0.001 M) with a volume ratio of 3:1:3:3—was transferred to the same volumetric flask, and D.I. water was added to reach a total of 25 mL. D.I. water of 2 mL was used in the same procedure as the blank. After 30 min, the solution in the volumetric flask was shaken vigorously to mix it well, and the absorption of light was measured at 620 nm. The F⁻ concentration was obtained based on a calibration curve using NaF as the standard.

Analysis of Fe^{2+} and total Fe concentrations

Fe^0 NPs were separated from the suspension after the reaction by precipitation for 30 min, followed by a magnetic field separation. Fe^{2+} and total Fe (i.e., Fe^{2+} and Fe^{3+} species) concentrations in the supernatant were analyzed by the Ferrozine method using a UV–vis spectrophotometer (Viollier et al. 2000). Briefly, 100 μL of the supernatant after removal of the Fe^0 NPs was added into a cuvette, then 900 μL of D.I. water and 100 μL of the Ferrozine solution (0.01 M) were added. The absorbance was recorded at 562 nm after 10 min to test the Fe^{2+} concentration. Then, 150 μL of reducing agent $NH_2OH \cdot HCl$ (1.4 M in 2 M HCl solution) and 50 μL of NH_4Ac buffer (10 M, pH 9.5) were added in the cuvette. The solution was allowed to react for 2 h to complete the reduction of Fe^{3+} to Fe^{2+}, and absorbance at 562 nm was recorded for the total Fe concentration. Fe^{2+} and the total Fe concentrations in the samples were obtained from their respective calibration curves, and the concentration of Fe^{3+} in each sample was obtained by the difference of the total Fe concentration and the Fe^{2+} concentration.

Determination of defluorination rate

The defluorination rate of PFOA was calculated by Eq. 1.

$$R = \frac{C_{F^-}}{\dfrac{15 \times C_0 \times 19}{414}} \times 100 \qquad (1)$$

R represents the defluorination rate of PFOA, %; C_{F^-} represents the concentration of F⁻ in solution, mg/L; C_0 represents the initial concentration of PFOA in solution, mg/L; the factor 15 corresponds to the number of fluorine atoms contained in one PFOA molecule, the factor 19 is the atomic weight of fluorine, and the factor 414 is the molecular weight of PFOA.

Results and discussion

Effect of light source on PFOA decomposition

Light source is critical for a photolytic process, as it provides photons absorbed by contaminants for their degradation (Li et al. 2017). Besides, hydrated electrons (e_{aq}^-), which have demonstrated excellent performance in cleaving C–F bonds, can be generated from H_2O or specific chemicals under UV irradiation (Bentel et al. 2019). UVC light (254 nm) was selected in this study and compared to visible light and dark conditions. Natural light, which contains only 3–4% UV light, was not tested. Under UVC (254 nm) light, removal of PFOA (1 mg/L) was detected and reached 58 ± 2.0% at 25 h (Fig. 1). In comparison, no PFOA removal was detected under visible light or in the dark in 25 h (Fig. 1). This was consistent with the discoveries in the literature that PFOA was not decomposed in the dark (Liu et al. 2013a), and direct photolysis was not possible for PFOA under visible light (Li et al. 2012). PFOA does not absorb visible light (Wang et al. 2017), but it has a weak and broad absorption of UV light from 220 to 270 nm (Hori et al. 2004). The result also indicated no PFOA adsorption happened in the reactor and during the sample preparation process. In this study, UV light intensity of 6.57 mW/cm² was used, which was low compared to the intensity reported in the literature of 17.57 mW/cm² (Thi et al. 2013); thus, the PFOA degradation process was less expensive but the degradation rate was comparatively lower. When the PFOA initial concentration was increased to 10 mg/L, it was barely degraded in 9 h,

then decomposed fast after 13 h, and the degradation rate of PFOA reached $45.8 \pm 6.5\%$ at 25 h (Fig. 2). With the same intensity of UV irradiation, the PFOA degradation rate was lower for 10 mg/L compared to 1 mg/L (Figs. 1 and 2); this should be due to the increased concentration of PFOA that required more photons for its degradation.

Decomposition of PFOA under UVC light with Fe^0 nanoparticles

The PFOA (10 mg/L) degradation rate under UV light irradiation alone was close to that achieved at 25 h in the UV/Fe^0 system using 100 mg/L of Fe^0 NPs (with or without 1% PVP coating) (Fig. 2). However, the defluorination rate of the control (i.e., under UV light alone) was only $9.6 \pm 0.1\%$ after 25 h, which was $44.0 \pm 11.3\%$ and $41.7 \pm 1.7\%$ lower than adding 100 mg/L of Fe^0 NPs with or without 1% PVP coating, respectively (Fig. 3). In addition, higher PFOA degradation rates were reached at 6 h using bare Fe^0 NPs, and at 13 h using both bare and 1% PVP-coated Fe^0 NPs, compared to the control (Fig. 2). These increased rates should be related to PFOA photocatalytic degradation brought by the released Fe^{3+} ions from Fe^0 oxidation in the presence of oxygen (Eqs. 2–4, Fig. 4b) (Wang et al. 2017; Joo et al. 2004; Chang et al. 2011). Following the release of Fe^{2+} and Fe^{3+} ions after Fe^0 oxidation (Eqs. 2–4, Fig. 4) (Chen et al. 2017; Litter Marta and Slodowicz 2017; Rezaei and Vione 2018), the concentrations of Fe^{3+} ions reduced

from 12 h, while the concentrations of Fe^{2+} ions slightly increased or kept the same during the whole reaction (Fig. 4b), which indicated the possible formation of the $[C_7F_{15}COO\text{-}Fe]^{2+}$ complex from the dissociated PFO^- and Fe^{3+} (Eq. 5). Formation of this complex was also indicated from testing the UV–vis spectra of PFOA, $FeCl_3$, and the mixture of the two compounds: the absorption spectrum of the mixture of PFOA and $FeCl_3$ was similar to that of $FeCl_3$, but the absorption intensity was lower for the mixture of PFOA and $FeCl_3$ compared to the intensity of $FeCl_3$ alone (see Fig. S5 in Supporting Information). The same phenomenon was also observed in a previous study (Wang et al. 2008). In comparison, the absorption spectra of $FeCl_2$ alone and the mixture of PFOA and $FeCl_2$ were almost coincident (see Fig. S5 in Supporting Information), which indicated negligible complex formation between PFO^- and Fe^{2+}. The formed $[C_7F_{15}COO\text{-}Fe]^{2+}$ complex could be decomposed to Fe^{2+}, an organic alkyl radical $C_7F_{15}\cdot$, and CO_2 under UVC irradiation (Eq. 6) (Wang et al. 2017). And the alkyl radical may react with water to form unstable $C_7F_{15}OH$, which could further react with water to form PFHpA and release hydrofluoric acid (HF) for defluorination (Eqs. 7 and 8) (Wang et al. 2008; Thi et al. 2013; Wang et al. 2017; Trojanowicz et al. 2018). The same loop of reaction would carry on for PFHpA to form PFHxA and release HF and CO_2. Eventually, CO_2 and HF would be the final products of PFOA mineralization. Schematic mechanism illustrations of PFOA degradation by Fe^0 NPs under UVC light are shown in Fig. 5.

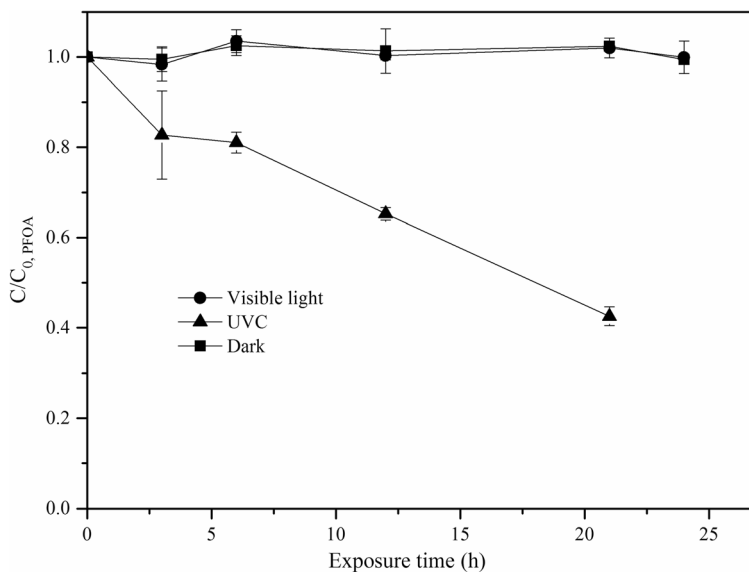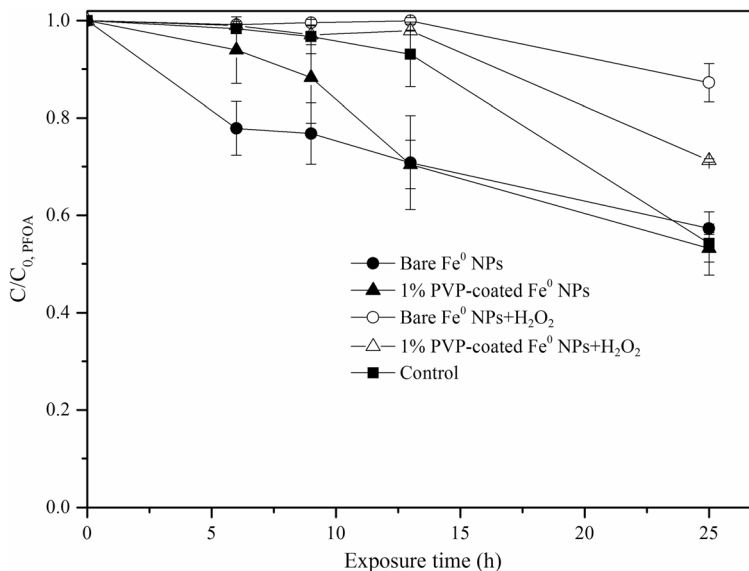Fig. 1 PFOA removal under UVC (254 nm) light, visible light, and in the dark after 25 h. $C_{0, PFOA}$ = 1 mg/L

Fig. 2 Change in PFOA concentration with time under UVC irradiation by Fe^0 NPs without or with H_2O_2. $C_{0, PFOA} = 10$ mg/L, $C_{0, Fe^0} = 100$ mg/L, $C_{0,H_2O_2} = 30$ mM

For 1 mg/L of PFOA, the concentration of PFOA decreased rapidly in the first 3 h, then it went up, which indicated possible PFOA adsorption removal by bare Fe^0 NPs in the initial stage (see Fig. S3 in Supporting Information). In comparison, for higher concentration of 10 mg/L of PFOA, this phenomenon of PFOA concentration decrease then increase was minimized (Fig. 2), which indicated likely concentration and time-dependent sorption removal of PFOA by the UV/Fe^0 system. PFOA removal by adsorption was also reported in previous studies using Fe^0 NPs (Arvaniti et al. 2015; Baldwin 2018; Liu et al. 2017).
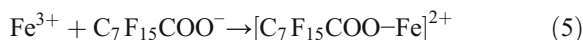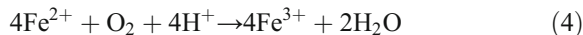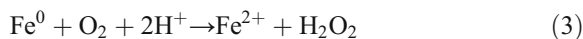
$$2Fe^0 + O_2 + 4H^+ \rightarrow 2Fe^{2+} + 2H_2O \qquad (2)$$

$$Fe^0 + O_2 + 2H^+ \rightarrow Fe^{2+} + H_2O_2 \qquad (3)$$

$$4Fe^{2+} + O_2 + 4H^+ \rightarrow 4Fe^{3+} + 2H_2O \qquad (4)$$

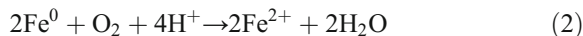$$Fe^{3+} + C_7F_{15}COO^- \rightarrow [C_7F_{15}COO-Fe]^{2+} \qquad (5)$$
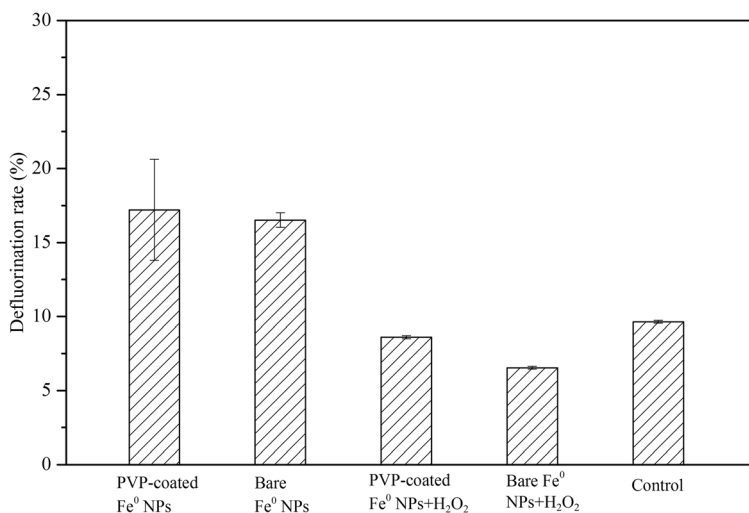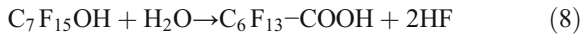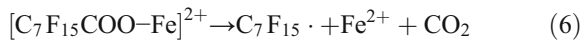
Fig. 3 PFOA defluorination rates after 25 h reaction under UVC irradiation by Fe^0 NPs without or with H_2O_2. $C_{0, PFOA} = 10$ mg/L, $C_{0, Fe^0} = 100$ mg/L, $C_{0,H_2O_2} = 30$ mM

$$[C_7F_{15}COO-Fe]^{2+} \rightarrow C_7F_{15} \cdot + Fe^{2+} + CO_2 \qquad (6)$$

$$C_7F_{15} \cdot + H_2O \rightarrow C_7F_{15}OH + H \qquad (7)$$

$$C_7F_{15}OH + H_2O \rightarrow C_6F_{13}-COOH + 2HF \qquad (8)$$

Impact of coating of Fe^0 nanoparticles on PFOA degradation

The degradation rate of PFOA using bare Fe^0 NPs was higher than that using 1% PVP-coated Fe^0 NPs in the initial 6 h, although the difference was diminished afterwards (Fig. 2). After 13 h, the degradation rate of PFOA was the same using either bare or 1% PVP-coated Fe^0 NPs (Fig. 2). One reason should be that some of the active reaction sites on the surface of Fe^0 NPs were blocked by the PVP coating, which would lead to reduced generation of Fe^{2+}, then Fe^{3+} in the initial stage (i.e., 6 h) during PFOA degradation (Fig. 4). In fact, the concentrations of Fe^{3+} and Fe^{2+} were both higher in the entire reaction duration using bare Fe^0 NPs compared to using 1% PVP-coated Fe^0 NPs (Fig. 4). The Fe^{2+} concentrations increased to 2.77 and 0.75 mg/L after 24 h; in comparison, the Fe^{3+} concentrations increased first to

Fig. 4 Fe^{2+} (**a**) and Fe^{3+} (**b**) concentrations in the supernatant after 24 h of PFOA reaction under UVC irradiation using Fe^0 NPs without or with H_2O_2. $C_{0,\,PFOA} = 10$ mg/L, $C_{0,\,Fe^0} = 100$ mg/L, $C_{0,H_2O_2} = 30$ mM
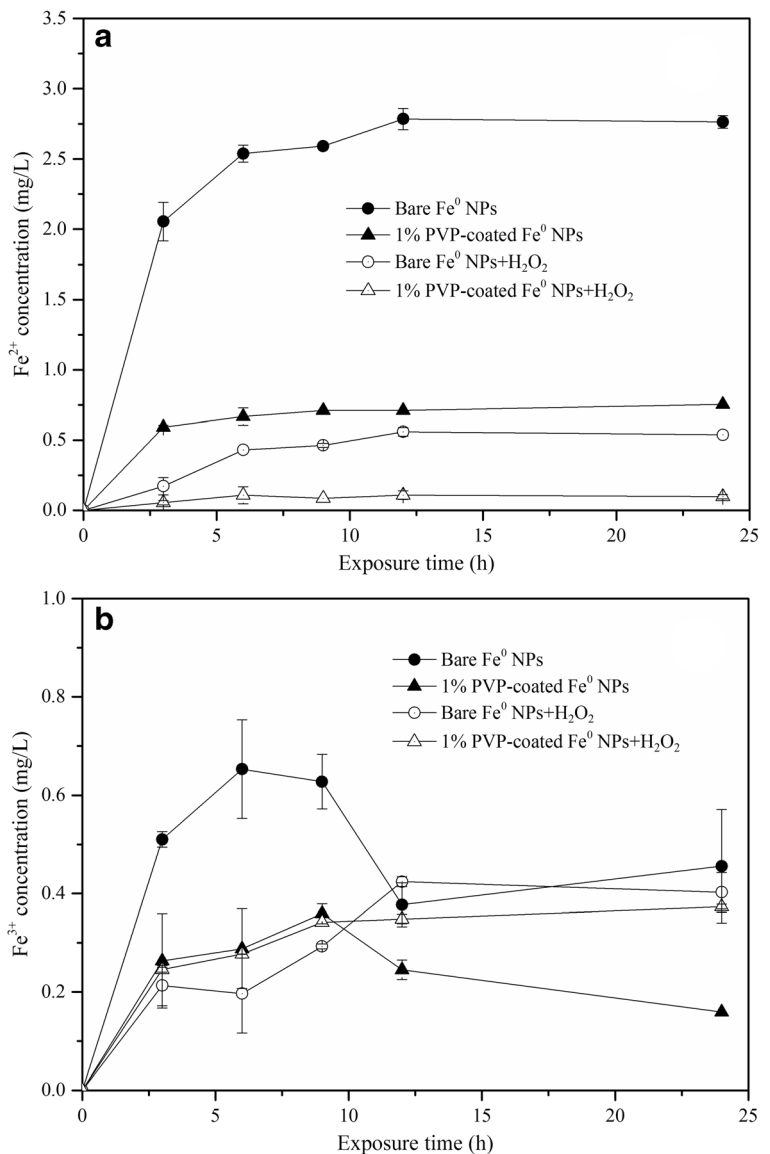
0.65 and 0.34 mg/L, then decreased to 0.46 and 0.16 mg/L after 24 h, using bare and 1% PVP-coated Fe^0 NPs, respectively (Fig. 4). Compared to the coated Fe^0 NPs, the uncoated Fe^0 NPs were more active in Fe^0 oxidation reaction. In the later stage, i.e., after 6 h, the surface of bare Fe^0 NPs would partially be covered by iron oxyhydroxides, formed from Fe^0 oxidation, thus reducing the difference in reactivity between bare and 1% PVP-coated Fe^0 NPs (see Fig. S6 in Supporting Information). Therefore, the difference of PFOA degradation in the later stage between the two types of NPs was diminished. Besides, the averaged smaller size of the lab-produced bare Fe^0 NPs compared to the purchased PVP-coated Fe^0 NPs (see Section S1.1. and Figs. S1 and S2 in Supporting Information) can provide a larger surface area for the bare NPs for PFOA degradation in the initial stage.

Decomposition of PFOA under UVC light with Fe^0 nanoparticles and H_2O_2

A lower degradation rate of PFOA was reached in the UV/Fe^0/H_2O_2 system compared to the control (i.e., under UVC light alone), with only 12.8–28.4% of PFOA degradation after 25 h (Fig. 2), and the defluorination rate of only 6.5–8.6% was also reduced compared to the control (Fig. 3). Besides, the concentrations of Fe^{2+} in 24 h as well as Fe^{3+}

in the initial 9 h in the UV/Fe^0/H_2O_2 system were also lower compared to those in the UV/Fe^0 system (Fig. 4), and the concentrations of Fe^{3+} in the UV/Fe^0/H_2O_2 system did not increase then decrease as those shown in the UV/Fe^0 system (Fig. 4); instead, Fe^{3+} concentrations kept increasing, which should be partly due to the oxidation of Fe^{2+} to Fe^{3+} by the presence of H_2O_2. Tiny bubbles were observed with H_2O_2 addition; these bubbles may be O_2 released by partial decomposition of H_2O_2. The presence of these tiny bubbles may slow down the formation of the [C7F15COO-Fe]$^{2+}$ complex consuming Fe^{3+} for PFOA degradation. The decreased PFOA degradation rate in the UV/Fe^0/H_2O_2 system may be also caused by the decreased UV utilization rate in the degradation process, as the UVC light could be used for H_2O_2 decomposition (Javed et al. 2020) to form ·OH, which is not effective in PFOA defluorination, but is capable of hydrogen atom abstraction from hydrocarbons (Hori et al. 2004; Cataldo 2014; Thi et al. 2013; Javed et al. 2020; Droege and Tully 1987).

PFOA degradation intermediates

PFOA degradation intermediates of PFHpA, PFHxA, and PFPeA were observed in all cases under UVC light (Fig. 6). PFBA was also observed under UVC light with or without 1% PVP-coated Fe^0 NPs (Fig. 6b–e). The molar fractions of the degradation intermediates to initial PFOA
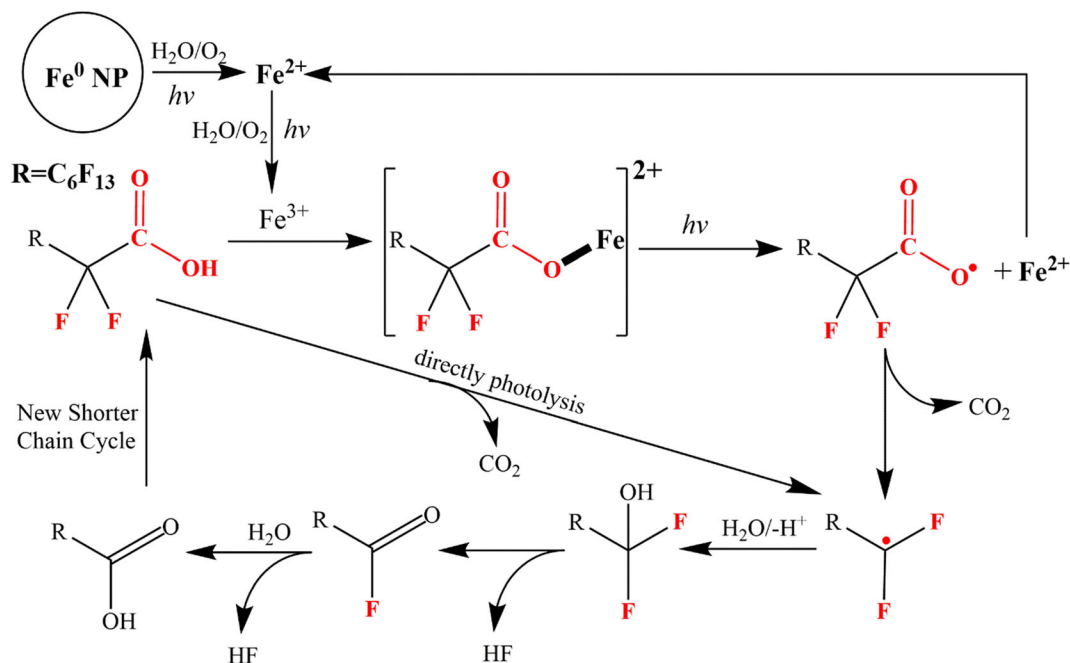

Fig. 5 Schematic mechanism illustrations of PFOA degradation by zero-valent iron nanoparticles (Fe^0 NPs) under UVC irradiation

increased in most cases with time using bare or 1% PVP-coated Fe[0] NPs without or with H_2O_2, as well as for the control (with only few cases reaching the plateau after 9 h) (Fig. 6). In particular, the molar fraction of PFHpA increased from 12.6% of the control to 28.6% and 15.8% for using bare and 1% PVP-coated Fe[0] NPs under UVC light, respectively, after 25 h (Fig. 6a–e). Besides, fluoride ions

were detected in all cases (Fig. 3), and the molar fractions of fluoride ions in PFCA intermediates to the initial PFOA are presented in Fig. S7 in Supporting Information. The generation of these intermediates proved PFOA degradation under UVC light with or without Fe[0] NPs, and agreed well with PFOA removal under each case. Two pathways were recently proposed for PFOA degradation upon
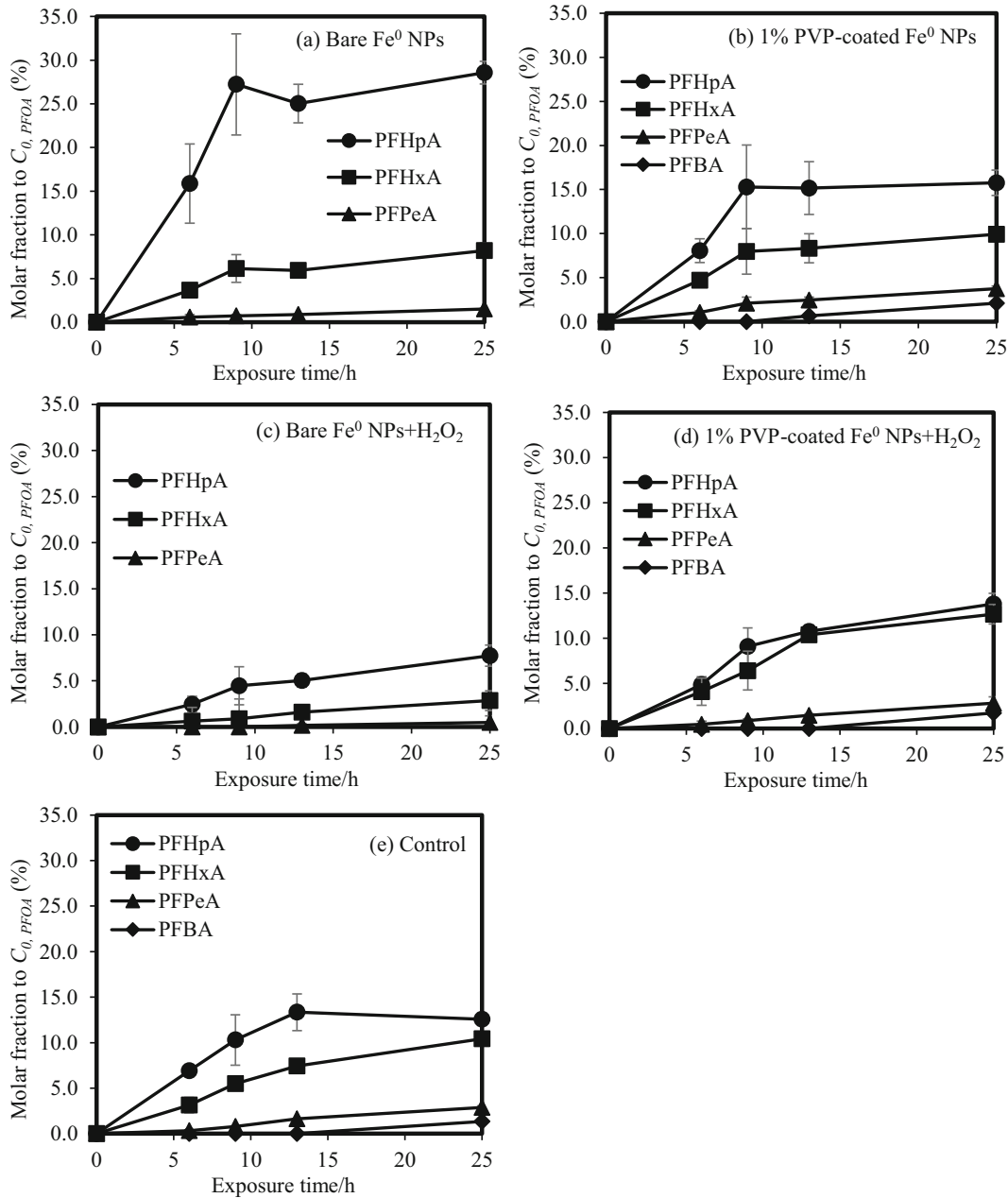

Fig. 6 Changes in molar fractions of degradation intermediates (i.e., PFHpA, PFHxA, PFPeA, and PFBA) to initial PFOA with time under UVC irradiation by Fe[0] NPs without or with H_2O_2. $C_{0, PFOA}$ = 10 mg/L (24.2 µM), $C_{0, Fe}^{0}$ = 100 mg/L, C_{0,H_2O_2} = 30 mM

reaction with hydrated electrons (e_{aq}^-) generated from H_2O or specific chemicals under UV irradiation: one is the decarboxylation–hydroxylation–elimination–hydrolysis (DHEH) pathway; the other is the H/F exchange pathway (Bentel et al. 2019). The PFOA chain shortening and the accompanying F^- release pathway proposed in our study (Fig. 5) follow the four similar steps as in the DHEH pathway, except that the proposed pathway in our study was initiated from PFOA oxidation by transferring an electron of the carboxylate terminal group of PFOA to the Fe(III)–carboxylate complex (Wang et al. 2017).

The UV/Fe^0 system developed in this study is feasible for practical applications, since the concentrations of PFOA in most contaminated waters are low in the ppt (and some in ppb) scale: first, the F^- concentrations generated during the treatment process should be very low, e.g., lower than the maximum contaminant level of 2.0 mg/L of the U.S. National Secondary Drinking Water Regulations; second, studies have shown the reduced toxicity of shorter-chain PFCAs (Buhrke et al. 2013; Luz et al. 2019) that were generated during the PFOA degradation process; and last, the reaction time may be largely shortened for treating low concentrations of PFOA in contaminated environmental media. Indeed, a positive correlation exists between the carbon chain length of the PFCA and its cytotoxicity (Buhrke, Kibellus et al. 2013, Gomis et al. 2018, Anderson, Luz et al. 2019, Luz, Anderson et al. 2019). For example, it was reported that PFHxA is not carcinogenic, genotoxic, a selective reproductive or developmental toxicant, or an endocrine disruptor (Luz, Anderson et al. 2019). Besides, the element iron is environment friendly; even the sum of the concentrations of

Fe^{2+} and Fe^{3+} in the solution after 25 h reaction in treating 10 mg/L PFOA in this study was lower than the recommended maximum concentration of iron (5 mg/L) in continuously used irrigation waters to all soils (Pick 2011). Our previous study also showed Fe^0 nanoparticles of 100 mg/L did not adversely affect the growth of *Arabidopsis thaliana* (Liu, Weinholtz et al. 2017).

pH change

After the degradation reaction, the pH of the reaction solution reduced with the released HF from 4.8 at the start when only PFOA was dissolved in the solution, to a close value of 4.7 in the UV/Fe^0 system after 25 h (Fig. 7). In contrast, the pH was increased to 5.0–5.1 in the UV/Fe^0/H_2O_2 system, and the pH of the control kept unchanged (Fig. 7). As HF was released during PFOA degradation, the slightly reduced pH indicated better PFOA degradation. Meanwhile, since Fe^0 NPs could generate hydroxide when exposed to water and oxygen, this could potentially resist the trend of pH reduction during PFOA degradation, and may bring benefit to the treatment of PFOA-contaminated environmental media—the pH of which is normally in the neutral range.

Conclusion

PFOA degradation was investigated for the first time by using Fe^0 NPs under UVC light. It was found that the PFOA removal was accelerated in the initial hours (e.g., 13 h) by introducing Fe^0 NPs, without or with 1% PVP

Fig. 7 Comparison of the pH of the solution after 25 h reaction under UVC irradiation by Fe^0 NPs without or with H_2O_2. $C_{0, PFOA}$ = 10 mg/L, C_{0, Fe^0} = 100 mg/L, C_{0,H_2O_2} = 30 mM
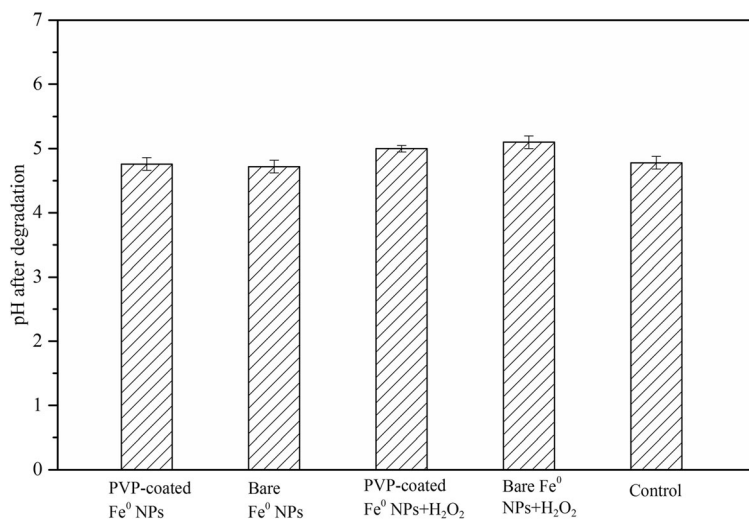
coating under UVC light, whereas no PFOA removal was observed either under visible light or in the dark. Moreover, the degradation rate using bare Fe^0 NPs was higher than that using 1% PVP-coated Fe^0 NPs in the initial 6 h. PFHpA, PFHxA, PFPeA, and PFBA were detected as the main intermediates. F^-, Fe^{2+}, and Fe^{3+} ions were also detected in the UV/Fe^0 system. Rapid consumption of Fe^{3+} indicated the possible formation of the $[C_7F_{15}COO-Fe]^{2+}$ complex that could initiate PFOA degradation. Introducing H_2O_2 into the UV/Fe^0 system resulted in a lower PFOA degradation rate and defloration rate, which suggested that H_2O_2 may counterproductively consume UV irradiation and consequently hinder PFOA degradation. By using Fe^0 NPs, no extra anions would be introduced compared to using iron salts for PFOA degradation under UVC light. Besides, the low toxicity and low cost of Fe^0 NPs, and easy removal of Fe^0 NPs by their magnetic properties from the treated water, made the technology of PFOA degradation by UV/Fe^0 attractive. Further studies are necessary exploring the application of Fe^0 NPs under UVC light to degrade PFOA in contaminated surface water and groundwater.

Compliance with ethical standards

Conflict of interest The authors declare that they have no conflict of interest.

References

Ahrens L (2011) Polyfluoroalkyl compounds in the aquatic environment: a review of their occurrence and fate. J Environ Monit 13:20–31

Ahrens L, Bundschuh M (2014) Fate and effects of poly- and perfluoroalkyl substances in the aquatic environment: a review. Environ Toxicol Chem 33:1921–1929

Anderson JK, Luz AL, Goodrum P, Durda J (2019) Perfluorohexanoic acid toxicity, part II: application of human health toxicity value for risk characterization. Regul Toxicol Pharmacol 103:10–20

Arvaniti OS, Hwang Y, Andersen HR, Stasinakis AS, Thomaidis NS, Aloupi M (2015) Reductive degradation of perfluorinated compounds in water using Mg-aminoclay coated nanoscale zero valent iron. Chem Eng J 262:133–139

Baldwin JR (2018) Evaluation of the removal of perfluoroalkyl substances from aqueous matrices in the presence of zerovalent iron. UWSpace http://hdl.handle.net/10012/12875

Bautitz IR, Velosa AC, Nogueira RF (2012) Zero valent iron mediated degradation of the pharmaceutical diazepam. Chemosphere 88:688–692

Bentel MJ, Yu Y, Xu L, Li Z, Wong BM, Men Y, Liu J (2019) Defluorination of per- and polyfluoroalkyl substances (PFASs) with hydrated electrons: structural dependence and implications to PFAS remediation and management. Environ Sci Technol 53(7):3718–3728

Bruton TA, Sedlak DL (2018) Treatment of perfluoroalkyl acids by heat-activated persulfate under conditions representative of in situ chemical oxidation. Chemosphere 206:457–464

Buck RC, Franklin J, Berger U, Conder JM, Cousins IT, De Voogt P, Jensen AA, Kannan K, Mabury SA, Leeuwen SP (2011) Perfluoroalkyl and polyfluoroalkyl substances in the environment: terminology, classification, and origins. Integr Environ Assess Manag 7(4):513–541

Buhrke T, Kibellus A, Lampen A (2013) In vitro toxicological characterization of perfluorinated carboxylic acids with different carbon chain lengths. Toxicol Lett 218(2):97–104

Cataldo F (2014) Hydrogen peroxide photolysis with different UV light sources including a new UV-LED light source. New Front in Chem 23(2):99–110

Chen J, Zhang P (2006) Photodegradation of perfluorooctanoic acid in water under irradiation of 254 nm and 185 nm light by use of persulfate. Wat Sci Tech 54(11–12):317–325

Chen J, Zhang P, Liu J (2007) Photodegradation of perfluorooctanoic acid by 185 nm vacuum ultraviolet light. J Environ Sci 19:387–390

Chen X, Ji D, Wang X, Zang L (2017) Review on nano zerovalent Iron (nZVI): from modification to environmental applications. IOP Conf Ser: earth environ Sci 50:012004 https://iopscience.iop.org/article/10.1088/1742-6596/51/1/012004

Cheng J, Vecitis CD, Park H, Mader BT, Hoffmann MR (2008) Sonochemical degradation of perfluorooctane sulfonate (PFOS) and perfluorooctanoate (PFOA) in landfill groundwater: environmental matrix effects. Environ Sci Technol 42:8057–8063

Dutta AK, Maji SK, Adhikary B (2014) γ-Fe2O3 nanoparticles: an easily recoverable effective photo-catalyst for the degradation of rose bengal and methylene blue dyes in the wastewater treatment plant. Mater Res Bull 49:28–34

Droege AT, Tully FP (1987) Hydrogen-atom abstraction from alkanes by hydroxyl radical. 6. Cyclopentane and cyclohexane. J Phys Chem 91(5):1222–1225

Environmental Protection Standard of China HJ 488-2009 (2009) Water quality—determination of fluoride—fluorine reagents spectrophotometry. https://www.codeofchina.com/standard/HJ488-2009.html

Eschauzier C, Beerendonk E, Scholte-Veenendaal P, De Voogt P (2012) Impact of treatment processes on the removal of perfluoroalkyl acids from the drinking water production chain. Environ Sci Technol 46:1708–1715

Fernandez NA, Rodriguez-Freire L, Keswani M, Sierra-Alvarez R (2016) Effect of chemical structure on the sonochemical degradation of perfluoroalkyl and polyfluoroalkyl substances (PFASs). Environ Sci-Wat Res 2:975–983

Flores C, Ventura F, Martin-Alonso J, Caixach J (2013) Occurrence of perfluorooctane sulfonate (PFOS) and perfluorooctanoate (PFOA) in N.E. Spanish surface waters and their removal in a drinking water treatment plant that combines conventional and advanced treatments in parallel lines. Sci Total Environ 461-462:618–626

Gehrke I, Geiser A, Somborn-Schulz A (2015) Innovations in nanotechnology for water treatment. Nanotechnol Sci Appl 8:1–17

Giesy JP, Kannan K (2002) Peer reviewed: Perfluorochemical surfactants in the environment. Environ Sci Technol 36(7): 146A–152A

Giri RR, Ozaki H, Morigaki T, Taniguchi S, Takanami R (2011) UV photolysis of perfluorooctanoic acid (PFOA) in dilute aqueous solution. Wat Sci Tech 63(2):276–282

Gomez-Ruiz B, Ribao P, Diban N, Rivero MJ, Ortiz I, Urtiaga A (2018) Photocatalytic degradation and mineralization of perfluorooctanoic acid (PFOA) using a composite TiO_2−rGO catalyst. J Hazard Mater 344:950–957

Gomis MI, Vestergren R, Borg D, Cousins IT (2018) Comparing the toxic potency in vivo of long-chain perfluoroalkyl acids and fluorinated alternatives. Environ Int 113:1–9

Hori H, Hayakawa E, Einaga H, Kutsuna S, Koike K, Ibusuki T, Kiatagawa H, Arakawa R (2004) Decomposition of environmentally persistent perfluorooctanoic acid in water by photochemical approaches. Environ Sci Technol 38:6118–6124

Houde M, De Silva AO, Muir DCG, Letcher RJ (2011) Monitoring of perfluorinated compounds in aquatic biota: an updated review. Environ Sci Technol 45:7962–7973

Houtz EF, Higgins CP, Field JA, Sedlak DL (2013) Persistence of perfluoroalkyl acid precursors in AFFF-impacted groundwater and soil. Environ Sci Technol 47:8187–8195

Iavicoli I, Leso V, Fontana L, Calabrese EJ (2018) Nanoparticle exposure and hormetic dose–responses: an update. Int J Mol Sci 19(3):805

Javed H, Lyu C, Sun R, Zhang D, Alvarez PJJ (2020) Discerning the inefficacy of hydroxyl radicals during perfluorooctanoic acid degradation. Chemosphere 247:125883

Jin L, Zhang P, Shao T, Zhao S (2014) Ferric ion mediated photodecomposition of aqueous perfluorooctane sulfonate (PFOS) under UV irradiation and its mechanism. J Hazard Mater 271:9–15

Joo SH, Feitz AJ, Waite TD (2004) Oxidative degradation of the carbothioate herbicide, molinate, using nanoscale zero-valent iron. Environ Sci Technol 38:2242–2247

Laine DF, Blumenfeld A, Cheng IF (2008) Mechanistic study of the ZEA organic pollutant degradation system: evidence for H_2O_2, HO•, and the homogeneous activation of O_2 by $Fe^{II}EDTA$. Ind Eng Chem Res 47:6502–6508

Lawal WA, Choi H (2018) Feasibility study on the removal of perfluorooctanoic acid by using palladium-doped nanoscale zerovalent iron. J Environ Eng 144:04018115

Li M, Wen D, Qiang Z, Kiwi J (2017) VUV/UV light inducing accelerated phenol degradation with a low electric input. RSC Adv 7(13):7640–7647

Li X, Zhang P, Jin L, Shao T, Li Z, Cao J (2012) Efficient photocatalytic decomposition of perfluorooctanoic acid by indium oxide and its mechanism. Environ Sci Technol 46: 5528–5534

Li Z, Zhang P, Shao T, Wang J, Jin L, Li X (2013) Different nanostructured In_2O_3 for photocatalytic decomposition of perfluorooctanoic acid (PFOA). J Hazard Mater 260:40–46

Litter Marta I, Slodowicz M (2017) An overview on heterogeneous Fenton and photoFenton reactions using zerovalent iron materials. J Adv Oxid Technol 20(1):20160164

Liu D, Xiu Z, Liu F, Wu G, Adamson D (2013a) Perfluorooctanoic acid degradation in the presence of Fe(III) under natural sunlight. J Hazard Mater 262:456–463

Liu J, Vipulanandan C, Cooper TF, Vipulanandan G (2013b) Effects of Fe nanoparticles on bacterial growth and biosurfactant production. J Nanopart Res 15:1405

Liu J, Vipulanandan C (2013) Effects of Au/Fe and Fe nanoparticles on Serratia bacterial growth and production of biosurfactant. Mater Sci Eng C Mater Biol Appl 33(7): 3909–3915

Liu J, Weinholtz L, Zheng L, Peiravi M, Wu Y, Chen D (2017) Removal of PFOA in groundwater by Fe^0 and MnO_2 nanoparticles under visible light. J Environ Sci Health A Tox Hazard Subst Environ Eng 52(11):1048–1054

Luz AL, Anderson JK, Goodrum P, Durda J (2019) Perfluorohexanoic acid toxicity, part I: development of a chronic human health toxicity value for use in risk assessment. Regul Toxicol Pharmacol 103:41–55

Mark R, Wiesner JYB (2017) Nanomaterials for groundwater remediation. In: Lowry GV (ed) Environmental nanotechnology: applications and impacts of nanomaterials, 2nd edn. McGraw-Hill, New York, pp 227–249

Moriwaki H, Takagi Y, Tanaka M, Tsuruho K, Okitsu K, Maeda Y (2005) Sonochemical decomposition of perfluorooctane sulfonate and perfluorooctanoic acid. Environ Sci Technol 39:3388–3392

Park S, Zenobio JE, Lee LS (2018) Perfluorooctane sulfonate (PFOS) removal with Pd^0/nFe^0 nanoparticles: adsorption or aqueous Fe-complexation, not transformation? J Hazard Mater 342:20–28

Pick T (2011) Assessing water quality for human consumption, agriculture, and aquatic life uses. Montana, USA, United States Department of Agriculture:1–31

Rezaei F, Vione D (2018) Effect of pH on zero valent iron performance in heterogeneous Fenton and Fenton-like processes: a review. Molecules (Basel, Switzerland) 23(12): 3127

Rhoads KR, Janssen EML, Luthy RG, Criddle CS (2008) Aerobic biotransformation and fate of n-ethyl perfluorooctane sulfonamidoethanol (N-EtFOSE) in activated sludge. Environ Sci Technol 42:2873–2878

Schaefer CE, Andaya C, Urtiaga A, McKenzie ER, Higgins CP (2015) Electrochemical treatment of perfluorooctanoic acid (PFOA) and perfluorooctane sulfonic acid (PFOS) in groundwater impacted by aqueous film forming foams (AFFFs). J Hazard Mater 295:170–175

Schröder HF, Meesters RJW (2005) Stability of fluorinated surfactants in advanced oxidation processes—a follow up of

degradation products using flow injection–mass spectrometry, liquid chromatography–mass spectrometry and liquid chromatography–multiple stage mass spectrometry. J Chromatogr A 1082(1):110–119

Shimada K, Shimoda T, Kokusen H, Nakano S (2005) Automatic microdistillation flow-injection system for the spectrophotometric determination of fluoride. Talanta 66(1):80–85

Takagi S, Adachi F, Miyano K, Koizumi Y, Tanaka H, Watanabe I, Tanabe S, Kannan K (2011) Fate of perfluorooctanesulfonate and perfluorooctanoate in drinking water treatment processes. Water Res 45(13):3925–3932

Tian H, Liang Y, Yang D, Sun Y (2020) Characteristics of PVP-stabilised NZVI and application to dechlorination of soil-sorbed TCE with ionic surfactant. Chemosphere 239:124807

Tang H, Xiang Q, Lei M, Yan J, Zhu L, Zou J (2012) Efficient degradation of perfluorooctanoic acid by UV–Fenton process. Chem Eng J 184:156–162

Thi LAP, Do HT, Lee YC, Lo SL (2013) Photochemical decomposition of perfluorooctanoic acids in aqueous carbonate solution with UV irradiation. Chem Eng J 221:258–263

Trojanowicz M, Bojanowska-Czajka A, Bartosiewicz I, Kulisa K (2018) Advanced oxidation/reduction processes treatment for aqueous perfluorooctanoate (PFOA) and perfluorooctanesulfonate (PFOS) – a review of recent advances. Chem Eng J 336:170–199

Viollier E, Inglett PW, Hunter K, Roychoudhury AN, Van Cappellen P (2000) The ferrozine method revisited: Fe(II)/Fe(III) determination in natural waters. Appl Geochem 15(6):785–790

Wang S, Yang Q, Chen F, Sun J, Luo K, Yao F, Wang X, Wang D, Li X, Zeng G (2017) Photocatalytic degradation of perfluorooctanoic acid and perfluorooctane sulfonate in water: a critical review. Chem Eng J 328:927–942

Wang Y, Zhang P, Pan G, Chen H (2008) Ferric ion mediated photochemical decomposition of perfluorooctanoic acid (PFOA) by 254nm UV light. J Hazard Mater 160:181–186

Xiao F (2017) Emerging poly- and perfluoroalkyl substances in the aquatic environment: a review of current literature. Water Res 124:482–495

Ye S, Yan M, Tan X, Liang J, Zeng G, Wu H, Song B, Zhou C, Yang Y, Wang H (2019a) Facile assembled biochar-based nanocomposite with improved graphitization for efficient photocatalytic activity driven by visible light. Appl Catal B 250:78–88

Ye S, Zeng G, Wu H, Liang J, Zhang C, Dai J, Xiong W, Song B, Wu S, Yu J (2019b) The effects of activated biochar addition on remediation efficiency of co-composting with contaminated wetland soil. Resour Conserv Recycl 140:278–285

Zhao B, Zhang P (2009) Photocatalytic decomposition of perfluorooctanoic acid with β-Ga$_2$O$_3$ wide bandgap photocatalyst. Catal Commun 10(8):1184–1187

Zhao X, Xia J, Chen W, Chen Y, Fang Y, Qu F (2019) Transport characteristics of salt ions in soil columns planted with Tamarix chinensis under different groundwater levels. PLoS One 14(4):e0215138